HHS Public Access

Author manuscript

Clin Cancer Res. Author manuscript; available in PMC 2022 May 15.

Published in final edited form as:

Clin Cancer Res. 2021 November 15; 27(22): 6174–6183. doi:10.1158/1078-0432.CCR-21-0987.

Spatial mapping and immunomodulatory role of the OX40/OX40L pathway in human non-small cell lung cancer.

Angelo Porciuncula[1], **Micaela Morgado**[1], **Richa Gupta**[1], **Kostas Syrigos**[2], **Robert Meehan**[3], **Sima J. Zacharek**[3], **Joshua P. Frederick**[3], **Kurt A. Schalper**[1,*]

[1]Department of Pathology, Yale University School of Medicine

[2]Oncology Unit, Department of Medicine, Athens University, Athens, Greece

[3]Moderna, Inc

Abstract

Purpose: To evaluate the tissue distribution and clinical significance of OX40 and OX40L in human non-small cell lung cancer (NSCLC).

Experimental Design: Using multiplexed quantitative immunofluorescence (QIF), we conducted simultaneous and localized measurements of OX40 and OX40L proteins, major T-cell subsets and conventional type-1 dendritic cells (cDC1) in 614 primary NSCLCs from three independent cohorts represented in tissue microarrays. We also measured OX40L protein in samples from a phase-I clinical trial of intratumor administration of a lipid nanoparticle encapsulated mRNA encoding OX40L (mRNA-2416) in human solid tumors. Finally, we studied the OX40 pathway in 212 uterine/ovarian serous carcinomas.

Results: OX40 protein was expressed in ~90% of NSCLCs and OX40L was detected in ~10% of cases. Increased expression of OX40 was associated with higher CD4+ and CD8+ T-lymphocytes, as well as cDC1s. Elevated expression of OX40L was consistently associated with increased CD4+ TILs and longer overall survival. No association was found between OX40 or OX40L levels and oncogenic driver mutations in EGFR and KRAS in lung adenocarcinomas. Delivering OX40L mRNA using intratumor mRNA-2416 injection mediated increased local OX40L protein levels that was most prominent in a patient with ovarian serous carcinoma. Detectable OX40L protein levels were observed in 15% of primary uterine/ovarian serous malignancies and associated with longer survival.

Conclusions: The OX40 pathway is expressed in a fraction of NSCLCs and is associated with a favorable immune contexture. Although OX40L is uncommonly expressed in NSCLC and serous malignancies, it is associated with better prognosis and can be introduced using exogenous mRNA.

[*]**Corresponding Author:** Kurt A. Schalper, MD, PhD, 310 Cedar Street, PO Box 208023, New Haven, CT, 06520-8023, United States, (203)-785-4719, kurt.schalper@yale.edu.

INTRODUCTION

The OX40/OX40L costimulatory pathway participates in adaptive immune responses by promoting T-cell proliferation and survival. OX40 (CD134; TNFRSF4), a member of the tumor-necrosis factor (TNF) superfamily, is expressed by activated T-cells upon antigen stimulation. Its subsequent ligation by OX40 ligand, or OX40L (CD134L; TNFSF4), expressed by mature antigen-presenting cells, protects T-cells from anergic cell death and promotes effector T-cell expansion and differentiation into a memory phenotype in the presence of a recognized antigen (1, 2). OX40L expression is stimulated by CD40/CD40L axis engagement, and cytokines including IL-18, TSLP, (1) and IFN-α (3). As shown by knockout studies, OX40 signaling is necessary for optimal clonal expansion of naïve $CD4^+$ T-cells and the generation of effective primary and memory $CD4^+$ T-cell responses (4, 5). Although OX40 pathway engagement appears to be dispensable in the generation of primary $CD8^+$ T-cell responses, it has been shown to regulate the generation and maintenance of $CD8^+$ memory T-cells in experimental models (6, 7). The OX40 pathway has also been shown to modulate regulatory T-cells in a context-dependent manner (8-10). Thus, the OX40/OX40L pathway is considered as a promising target to enhance adaptive anti-tumor immune responses.

OX40 agonism, particularly by the administration of monoclonal OX40 antibodies (mAbs), has led to tumor reduction in mice (11, 12) and induced modest clinical activity in humans (13, 14). Early clinical studies using these therapies as single agent showed that the treatment is well tolerated and, in one study, induced reduction in at least one metastatic lesion in 12 of 30 patients (13). A more recent dose-escalation study using a humanized OX40 IgG1 mAb to treat 50 patients with advanced solid tumors reported 2 partial responses and 22 cases with stable disease (14). Additional studies targeting the OX40 pathway using different strategies are ongoing (15-17).

In preclinical studies, the co-administration of OX40 mAbs and immune checkpoint blockers, such as PD-1 mAbs, has shown greater therapeutic efficacy than their monotherapy equivalents with some reports showing that timing of administration is an important consideration (18, 19). Given that several clinical trials are underway to test the efficacy of OX40 agonism in combination with other immunotherapies, a deeper understanding of the pathway, modulation strategies and the consequences of its stimulation in human cancer is required to optimally guide clinical development.

Here, we describe the expression, spatial distribution, immune and clinical features associated with the OX40/OX40L pathway in multiple non-small cell lung carcinoma (NSCLC) cohorts. We report marked differences in the expression of the receptor and ligand, as well as association between OX40/OX40L expression and a favorable tumor microenvironment characterized by increased T-lymphocytes, conventional type 1 dendritic cells (cDC1) and extended patient survival. We also describe a strategy to upregulate OX40L in human tumors using local delivery of exogenous OX40L mRNA and show proof-of-concept evidence in patients with advanced solid tumors. Similar to the observation in NSCLC, we also show a favorable prognostic impact of OX40L protein expression in primary uterine/ovarian serous malignancies.

MATERIALS AND METHODS

Patients and samples

Formalin-fixed paraffin-embedded (FFPE) tumor tissue samples from three retrospective collections of human NSCLCs represented in tissue microarrays (TMAs) were analyzed (20-22). TMAs were constructed including 2-4 individual 0.6 mm (diameter) cores from each tumor sample. The marker scores from all available tumor cores with >5% tumor area per case were averaged. The regions of interest (ROIs) from each case were selected by a trained pathologist to be representative of the lesion and each ROI was imaged using 20x magnification. The first cohort (Cohort 1) included samples from 280 patients with primary NSCLC treated at Yale-New Haven Hospital from 1988 to 2012; and the second cohort (Cohort 2) consisted of tumors from 207 patients from Greece collected between 1991 to 2001. Clinicopathologic information was available for both collections including age of diagnosis, gender, stage, histology, smoking status and survival (Supplementary Table S1). A third cohort (Cohort 3), comprising 127 primary lung adenocarcinomas from Yale-New Haven Hospital clinically tested for activating mutations in *EGFR* and *KRAS* was also analyzed. Additional samples included selected tumor lesions from patients with advanced solid malignancies enrolled in a phase I clinical trial (Moderna Inc, NCT03323398), at baseline and after intratumor treatment with a lipid nanoparticle (LNP)- encapsulated mRNA encoding OX40L (mRNA-2416), as well as a previously reported retrospective cohort (Cohort 4) of 212 primary ovarian and uterine serous carcinomas from Yale-New Haven Hospital (Supplementary Table S2) (23). This study was carried out in accordance with the principles of the Declaration of Helsinki and all tissue and clinical information were used in a de-identified fashion after approval from the Yale Internal Review Board (Yale Human Investigation Committee) protocols #9505008219 and #1608018220 or local institutional protocols, which approved the patient consent forms or waiver of consent.

Multiplexed quantitative immunofluorescence

Three multiplexed quantitative immunofluorescence (QIF) panels were standardized for simultaneous and spatially resolved measurement of OX40 and OX40L (DAPI/CK/OX40/OX40L), major T-cell subsets (DAPI/CK/CD4/CD8/FOXP3) (20) and cDC1 cells (DAPI/CK/CD11c/XCR1/HLA-DR) in the tumor cohorts. Additional panels were stained in a subset of NSCLC cases to map the expression of OX40 and OX40L in major T-cell subsets and relative to PD-L1 protein including: DAPI/CK/OX40/FOXP3/CD4, DAPI/CK/OX40L/FOXP3/CD4, DAPI/CK/PD-L1/OX40/OX40L, and DAPI/CK/OX40/OX40L/CD8.

The panels were stained in consecutive TMA sections, scored individually and data were integrated. Antibodies detecting human OX40 and OX40L were validated for specificity by analyzing their expression in Hep3B and HeLa cells transfected with OX40 cDNA and OX40L mRNA, respectively (Supplementary Figure S1c-f). According to laboratory protocols, cell lines were authenticated every 3–6 months.

Multiplexed QIF was performed as previously reported (20-22). Briefly, TMA sections were deparaffinized, rehydrated, and processed for antigen retrieval with 1 mM EDTA, pH 8.0 (Sigma-Aldrich) in a pressure-boiling module (Lab Vision) at 97°C for 20 minutes.

Slides were then incubated with methanol containing 0.75% hydrogen peroxide at room temperature (RT) for 30 minutes and subsequently in blocking solution containing 0.3% bovine serum albumin and 0.05% Tween 20 at RT for 30 minutes. Primary antibodies included: anti-OX40 (rabbit monoclonal IgG, clone SP195, Abcam; 1:200, 4°C overnight), anti-OX40L (rabbit monoclonal IgG, clone D6K7R, Cell Signaling Technology; 1:50, RT 1 hour), anti-HLA-DR (mouse monoclonal IgG2b, clone 4C8, LifeSpan Bio; 1:200, 4°C overnight), anti-CD11c (rabbit monoclonal IgG, clone D3VE1, Cell Signaling Technology; 1:200, 4°C overnight), anti-XCR1 (rabbit monoclonal IgG, clone D2F8T; 1:50, RT 1 hour), anti-CD4 (rabbit monoclonal IgG, clone SP35, Spring Biosciences; 1:100, RT 1 hour), anti-CD8 (mouse monoclonal IgG1k, clone C8/144B, Dako; 1:250, RT 1 hour), anti-FOXP3 (rabbit monoclonal IgG, clone D2W8E, Cell Signaling Technology; 1:25, RT 1 hour) and anti-PD-L1 (rabbit monoclonal IgG, clone E1L3N, Cell Signaling Technology; 1:800, 4°C overnight). All secondary antibodies were added at RT for 1 hour: anti-rabbit Envision (Dako), mouse anti-rabbit conjugated with horseradish peroxidase (HRP) (clone 2A9, Abcam; 1:200), goat polyclonal anti-mouse IgG2b conjugated with HRP (Abcam; 1:200), goat polyclonal anti-rabbit IgG conjugated with HRP (Abcam; 1:200), and rat anti-mouse IgG1k conjugated with HRP (clone M1-14D12, eBioscience; 1:100). Fluorophore-conjugated reagents were added subsequently after each primary-secondary antibody pair: Cy3-tyramide (Akoya Biosciences), Cy5-tyramide (Akoya Biosciences), and biotinylated tyramide (Akoya Biosciences) followed by streptavidin conjugated with Alexa Fluor 750 (Thermo Fisher). Residual HRP was quenched in-between incubations with secondary antibodies/fluorophores by treating the slides twice for 7 minutes with 1X PBS containing 0.136 g of benzoic hydrazide (Sigma) and 50 μl 30% (w/w) hydrogen peroxide. Tumor epithelial cells were stained for cytokeratin (CK) by incubating all slides with anti-CK (mouse monoclonal IgG1, clone AE1/AE3, eBioscience/Thermo; 1:200, RT 1 hour). Nuclei were counterstained with 4’,6-diamidino-2-phenylindole (DAPI). Washes were done with 1X TBS and 1X TBST (TBS with 0.1% Tween 20) after every application of reagent. An index TMA that was used in antibody titration for both markers was included in each run to assess reproducibility across experiments.

QIF analysis and scoring

Quantitative scanning, measurement, and analysis of fluorescent signal scores including both the number of positive cells and the marker intensity was performed by the AQUA® method of QIF (Navigate Biopharma) enabling detection of markers within user-defined compartments (20). Compartments were defined on the basis of CK positivity (tumor cells), CK negativity (stromal cells), and DAPI positivity (total; all nucleated cells). QIF scores were calculated by dividing the signal intensity of markers in a given compartment by the area of the compartment. Scores were normalized by exposure time and bit depth. Marker positivity was established by determining a visual detection threshold present in the cases and in positive and negative control samples.

Individual cell phenotyping based on co-expression of multiple markers and quantification of selected cell populations were performed using inForm software v.2.4.11 (Akoya Biosciences) on images scanned on the Vectra Polaris microscope (Akoya Biosciences).

Intratumoral administration of mRNA-2416

Patients with advanced and refractory tumors were injected with mRNA-2416, an LNP-encapsulated mRNA encoding human OX40L, in a phase I clinical trial (Moderna Inc, NCT03323398). Treatment was directly injected in non-visceral and clearly visible or palpable tumors. All lesions for initial injection were ≥ 0.5 cm on longest diameter and at least 5 mm thick. Tumor biopsies were collected at baseline and 24-48 hours after the first or third treatment. Samples were formalin-fixed for 14-24 hours, paraffin-embedded, and 5 μm sections analyzed by QIF.

Statistical analysis

QIF score comparisons were performed using Mann-Whitney test for two groups and Kruskal-Wallis test for three groups. Relationships between continuous scores were analyzed by Spearman correlation and those between categorical variables by Chi-square test. Survival analysis was performed by Mantel-Cox/log-rank test. P-values of <0.05 were considered significant using two-sided tests. Statistical analyses were performed using SPSS v.26 (IBM) and GraphPad Prism v.9.

RESULTS

OX40/OX40L expression in human NSCLC

We first assessed the expression of OX40 and OX40L protein in samples from two retrospective cohorts of human NSCLC (Cohort 1, n=280 and Cohort 2, n=207). The antibodies included in the QIF panels were validated and standardized using cell line transfectants and human tissue controls (Supplementary Figure S1). As shown in Figure 1a, we found a wide range of OX40/OX40L protein expression patterns that were maintained in comparable percentages between cohorts, including tumors showing virtual absence of either marker ($OX40^{low}OX40L^{low}$ in 10% and 12% in Cohorts 1 and 2, respectively), cases with predominant expression of one of the markers ($OX40^{high}OX40L^{low}$ in 81% and 74%; $OX40^{low}OX40L^{high}$ in 0% and 1%, respectively) and others with high co-expression of both ($OX40^{high}OX40L^{high}$ in 9% and 13% of cases).

OX40 displayed a membranous/cytoplasmic staining pattern and was detected almost exclusively in cytokeratin (CK)-negative stromal cells with morphological features consistent with lymphocytes and myeloid cells. Analysis of a subset of cases using additional QIF panels including OX40 and T-cell markers showed higher expression of OX40 in CD4+ helper T-cells and CD4+/FOXP3+ Tregs than in CD8+ effector populations (Supplementary Figure S5a-b). High OX40L signal was detected predominantly in CK^+ epithelial tumor cells with a cytoplasmic/membranous staining pattern and also focally in intratumor and neighboring CK^- stromal and immune cells (Figure 1a and Supplementary Figure S2).

In the quantitative analysis, OX40 and OX40L showed a continuous distribution across cases and limited association with each other (Figure 1b). Using the visual signal detection threshold as stratification cut-point, detectable levels of OX40 were identified in 90% of cases in Cohort 1 and 87% in Cohort 2 (Figure 1b). However, OX40L protein was detected

in only 9% of cases in Cohort 1 and 14% in Cohort 2 (Figure 1b). There was low correlation between the markers in both cohorts (Figure 1c). In the fluorescence signal quantification, the majority of OX40 protein signal was located in the CK^- stromal compartment, while OX40L levels were marginally higher in the tumor compartment (Figure 1d). Together, these results indicate that OX40 is commonly expressed in immune cells of the human NSCLC microenvironment, while OX40L is expressed in a relatively small fraction of cases, including both tumor and stromal/immune cells.

OX40/OX40L expression and immune contexture in NSCLC

In both NSCLC cohorts, higher expression of OX40 was significantly associated with increased $CD4^+$ TILs ($p<0.0001$, Cohort 1; and $p=0.0451$, Cohort 2) and $CD8^+$ TILs ($p=0.0354$, Cohort 1; and $p=0.0391$, Cohort 2) (Figure 2a). In Cohort 1, cases with higher OX40 levels also displayed lower $FOXP3^+$ regulatory T-cells (Tregs) ($p=0.0360$) (Supplementary Figure S3a), but this was not observed in Cohort 2. In contrast, high OX40L expression was consistently associated only with higher $CD4^+$ TILs (Figure 2a). Increased OX40L was also associated with lower Tregs and increased $CD20^+$ B cells in Cohort 1, but this was not seen in the second collection (Supplementary Figure S3a). The inconsistent association seen for Tregs and $CD20^+$ cells across the cohorts could be at least partially explained by the relatively low abundance and substantial intratumor variation of these cell subsets. Increased OX40 or OX40L was also associated with higher PD-L1 protein expression in NSCLCs (Supplementary Figure S5c)

In addition to their association with T-cells, enhanced expression of OX40 in the tumor samples was prominently associated with increased levels of XCR1, CD11c, and HLA-DR, markers of conventional type 1 dendritic cells (cDC1) known to mediate antigen cross-presentation and $CD8^+$ T-cell priming (Figure 2b and Supplementary Figure S3b) (24). Using multi-marker single-cell phenotyping, an increased proportion of $XCR1^+$ $CD11c^+$ $HLA\text{-}DR^+$ cells was identified in cases with high OX40 levels (Figure 2c-d), consistent with abundant cross-presenting cDC1 dendritic cells in these malignancies. No association was found between OX40L levels and cDC1 (Figure 2c).

OX40/OX40L expression, clinicopathologic variables, and outcomes in NSCLC

Using the visual detection threshold as stratification cut-point, there was no consistent association between OX40 or OX40L expression and any of the major clinicopathologic variables including patient age, gender, clinical stage, NSCLC histology, and smoking status (Tables 1-2 and Supplementary Figure S5d). Moreover, there was no association between OX40 or OX40L protein levels and the presence or absence of activating mutations in *EGFR* or *KRAS* in lung adenocarcinomas from Cohort 3 (Figure 3). Of note, none of the cases displaying high OX40L expression was EGFR-mutated (Figure 3b).

As shown in Figure 4a, OX40 levels were only marginally associated with a 5-year overall survival benefit in the first NSCLC cohort (Cohort 1), but the effect was not observed in the second cohort. However, elevated OX40L expression was significantly associated with longer 5-year overall survival in both NSCLC cohorts (Figure 4b, $p=0.0275$, Cohort 1; and $p=0.0366$, Cohort 2). In addition, elevated OX40L mRNA transcript levels were significantly

associated with longer survival in a large NSCLC collection (n=1,922) including cases from multiple databases including GEO, EGA (European Genome-phenome Archive) and The Cancer Genome Atlas (TCGA) (Supplementary Figure S5e).

Injection of OX40L transcript is associated with increased local OX40L protein production

As a proof-of-concept experiment, we analyzed baseline and on-treatment samples from patients with advanced solid tumors treated in a phase I/II clinical trial (NCT03323398) with at least one intratumoral injection of an LNP formulated mRNA encoding OX40L (i.e., mRNA-2416) as recently reported by Jimeno et al. (25). The extended results and safety profile from this clinical trial are pending independent publication. Analysis of core biopsy specimens by QIF demonstrated increased OX40L protein expression in 3 of 5 cases evaluated, indicative of local translation of the exogenous transcript into protein (Figure 5a-b). The most prominent increase was observed in a patient with advanced serous ovarian cancer (7.3-fold increase in pre vs post treatment, $p<0.0001$) (Figure 5b). To assess the expression and significance of the OX40 pathway in primary serous malignancies, we studied a retrospective collection of 212 patients with primary ovarian and uterine serous carcinomas (Cohort 4, Supplementary Figure S4). As shown in Figure 5c-d, OX40 protein was detected in 50% of cases and OX40L protein was identified in 15% of samples with predominant location in tumor epithelial cells. Consistent with a favorable prognostic role and similar to NSCLC, expression of OX40L protein was significantly associated with longer overall survival in this cohort (Figure 5f).

DISCUSSION

To our knowledge, this is the first report to spatially map and determine the clinical significance of the OX40 pathway in human NSCLC, including its association with other immune populations such as TIL subsets and cross-presenting cDC1 dendritic cells. The results indicate an imbalance between a relatively abundant OX40 receptor in immune cells and a limited local expression of its activating ligand, OX40L, in both lung carcinomas and ovarian/uterine serous malignancies. This points to OX40L as the limiting factor for pathway engagement and supports the rationale for stimulation of this pathway using agonistic monoclonal OX40 antibodies or OX40L-Fc fusion proteins (13, 26). Notably, our results also support exploiting the frequent absence of native OX40L expression by introducing the mRNA transcript exogenously and increasing local OX40L protein in the tumor microenvironment.

Our results indicate that OX40 expression is associated with a favorable tumor immune composition in NSCLC characterized by increased $CD4^+$ and $CD8^+$ T-cells, cDC1 dendritic cells and a modest positive prognostic effect that was inconsistent across the independent cohorts. The presence of increased TILs and cross-presenting dendritic cells is consistent with a more effective adaptive anti-tumor immune response. Specifically, cDC1 cells specialize in cross-presenting antigens to naïve $CD8^+$ T-cells, can stimulate $CD4^+$ T-cells and promote polarization toward a T helper 1 (Th1) phenotype (27). A recent report by Massarelli et al. (28) showed that high OX40 expression was associated with increased TILs and longer survival in a single cohort of 100 patients with NSCLCs. The apparent

differences in the magnitude of the effects seen in both studies could be due at least to the different tumor populations and dissimilar assays/platforms used for analysis.

Despite being expressed in a lower fraction of cases, OX40L showed a positive association with T-cell infiltration and a strong association with longer overall survival. This was seen in two independent NSCLC cohorts and in data from public mRNA databases, supporting the validity of the findings. This indicates that OX40L protein is uncommonly expressed in NSCLC, which could limit anti-tumor T-cell responses and is possibly under negative selective pressure in cancer cells and the tumor microenvironment. The similar findings seen in gynecologic serous carcinomas support that the expression and prognostic role of OX40L is not restricted to lung malignancies. However, the relatively low frequency of OX40L expression in the cohorts could limit the statistical power of these associations.

Interestingly, a prominent fraction of OX40L positivity occurs in tumor cells, suggesting an unexplored role for tumor-derived OX40L in modulating the immune response as has been described in other reports (29). Previous reports have shown that OX40 and/or OX40L expression associates with poor prognosis in hepatocellular carcinoma (30) and in lung malignancies (31). In these studies, the authors proposed that the OX40 pathway in cancer is associated with an immunosuppressive microenvironment driven by regulatory T-cells. Our data show that OX40 and OX40L expression are inconsistently associated with Tregs in NSCLC (Supplementary Figure S3a).

The therapeutic potential of OX40L mRNA was evidenced in our preliminary results after intratumoral administration of mRNA-2416 with the increase in local OX40L protein levels 24-48 hours post-treatment (25). Of note, the OX40L protein measurement in these cases was conducted using core biopsies that represent only a portion of the injected lesion; confirmed OX40L protein expression in all lesions injected with OX40L mRNA was observed in pre-clinical models in which whole tumors were assessed for expression (26). The phase I clinical trial of mRNA-2416 in solid tumors (NCT03323398) is still ongoing and the pharmacodynamic and clinical results are pending publication in a separate manuscript. This strategy can circumvent the low expression or absence of native OX40L in tumors and can favor a stronger and more physiological OX40 receptor ligation/signaling using endogenously produced OX40L oligomers. In addition, the intratumor administration of the transcript could potentially overcome some of the adverse events associated with systemic OX40 targeting antibodies such as ADCC-mediated immune cell depletion (32). The feasibility of this approach has been recently reported in pre-clinical models and early phase human clinical trials are ongoing (25). The pre-treatment expression levels of the OX40/OX40L pathway in tumors could potentially be used as selection criteria for such treatments.

Our study is not without limitations. First, we evaluated the samples in the retrospective cohorts using TMAs that analyze relatively small tissue fragments and might have over- or under-represented the marker measurements. However, the large number of cases analyzed and the use of multiple independent cohorts support the robustness of our findings. In addition, diverse reports from our group and others using TMAs have shown consistent results and significant association with clinicopathologic variables and outcomes using

this approach, supporting their reliability (20, 22, 33). Another possible limitation is the inclusion of retrospective cases treated in a non-controlled fashion in the retrospective cohorts. This is a common limitation of retrospective studies and their possible impact on the results is uncertain. Future studies using controlled model systems will be required to establish the mechanistic underpinnings of the immunostimulatory anti-cancer effect of the local OX40 pathway in cancer.

In summary, we have conducted a detailed analysis of the distribution and significance of the OX40 pathway using intact and clinically annotated tumor specimens. Our results reveal a dissimilar expression of OX40 and OX40L in NSCLC and primary serous carcinomas, as well as association with local adaptive anti-tumor responses in NSCLC. Our results also support a favorable prognostic role of OX40L protein expression in both NSCLC and ovarian/uterine malignancies and highlight the therapeutic potential of locally increasing OX40L using exogenous mRNA injection.

Supplementary Material

Refer to Web version on PubMed Central for supplementary material.

ACKNOWLEDGMENTS

This study was supported by the NIH grants R03CA219603 (K. Schalper), R37CA245154 (K. Schalper), Yale SPORE in Lung Cancer (P50CA196530), Stand Up To Cancer - American Cancer Society Lung Cancer Dream Team Translational Research Grants SU2C-AACR-DT17-15, Stand Up to Cancer Colorectal Cancer Dream Team Translational Research Grant SU2C-AACR-DT22-17, Mark Foundation EXTOL project 19-029-MIA, Yale Cancer Center Support Grant (P30CA016359) and sponsored research support by Moderna, Inc. Stand Up to Cancer is a division of the Entertainment Industry Foundation. The indicated SU2C grants are administered by the American Association for Cancer Research, the scientific partner of SU2C.

We would like to acknowledge David L. Rimm and Lori Charette from Yale Pathology Tissue Services for their excellent support for the TMA construction and histology processing, and Patricia Gaule from Yale Pathology Tissue Services for conducting the QIF analysis of mRNA-2416-treated samples. We would also like to acknowledge Maria Iliou and Ryan Millione for generating materials used for assay validation, and especially the patients and clinical study teams participating in the mRNA-2416-P101 trial.

Conflict of interest statement:

K.A.S. reports receiving research funding from Navigate Biopharma, Tesaro/GSK, Moderna Inc., Takeda, Surface Oncology, Pierre-Fabre Research Institute, Merck Sharpe & Dohme, Bristol-Myers Squibb, AstraZeneca, Ribon Therapeutics and Eli Lilly. In the last 24 months, K.A.S. has received honoraria for consultant/advisory or speaker roles from Shattuck Labs, Pierre-Fabre, EMD Serono, Clinica Alemana de Santiago, Genmab, PeerView, Fluidigm, Takeda/Millenium Pharmaceuticals, Merck Sharpe & Dohme, Bristol Myers-Squibb, Agenus and Torque Therapeutics. Robert Meehan, Sima Zacharek and Joshua Frederick are employees of Moderna Inc. Other authors do not report additional conflict of interest relevant for this work.

REFERENCES

1. Croft M, So T, Duan W, Soroosh P, The significance of OX40 and OX40L to T-cell biology and immune disease. Immunol Rev 229, 173–191 (2009). [PubMed: 19426222]
2. Sugamura K, Ishii N, Weinberg AD, Therapeutic targeting of the effector T-cell co-stimulatory molecule OX40. Nat Rev Immunol 4, 420–431 (2004). [PubMed: 15173831]
3. Kurche JS, Haluszczak C, McWilliams JA, Sanchez PJ, Kedl RM, Type I IFN-dependent T cell activation is mediated by IFN-dependent dendritic cell OX40 ligand expression and is independent of T cell IFNR expression. J Immunol 188, 585–593 (2012). [PubMed: 22156349]

4. Murata K et al. , Impairment of antigen-presenting cell function in mice lacking expression of OX40 ligand. J Exp Med 191, 365–374 (2000). [PubMed: 10637280]
5. Gramaglia I et al. , The OX40 costimulatory receptor determines the development of CD4 memory by regulating primary clonal expansion. J Immunol 165, 3043–3050 (2000). [PubMed: 10975814]
6. Lee SW et al. , Functional dichotomy between OX40 and 4-1BB in modulating effector CD8 T cell responses. J Immunol 177, 4464–4472 (2006). [PubMed: 16982882]
7. Bansal-Pakala P, Halteman BS, Cheng MH, Croft M, Costimulation of CD8 T cell responses by OX40. J Immunol 172, 4821–4825 (2004). [PubMed: 15067059]
8. Ruby CE et al. , Cutting Edge: OX40 agonists can drive regulatory T cell expansion if the cytokine milieu is right. J Immunol 183, 4853–4857 (2009). [PubMed: 19786544]
9. Takeda I et al. , Distinct roles for the OX40-OX40 ligand interaction in regulatory and nonregulatory T cells. J Immunol 172, 3580–3589 (2004). [PubMed: 15004159]
10. Polesso F, Sarker M, Weinberg AD, Murray SE, Moran AE, OX40 Agonist Tumor Immunotherapy Does Not Impact Regulatory T Cell Suppressive Function. J Immunol 203, 2011–2019 (2019). [PubMed: 31434709]
11. Piconese S, Valzasina B, Colombo MP, OX40 triggering blocks suppression by regulatory T cells and facilitates tumor rejection. J Exp Med 205, 825–839 (2008). [PubMed: 18362171]
12. Kjaergaard J et al. , Therapeutic efficacy of OX-40 receptor antibody depends on tumor immunogenicity and anatomic site of tumor growth. Cancer Res 60, 5514–5521 (2000). [PubMed: 11034096]
13. Curti BD et al. , OX40 is a potent immune-stimulating target in late-stage cancer patients. Cancer Res 73, 7189–7198 (2013). [PubMed: 24177180]
14. Glisson BS et al. , Safety and Clinical Activity of MEDI0562, a Humanized OX40 Agonist Monoclonal Antibody, in Adult Patients with Advanced Solid Tumors. Clin Cancer Res 26, 5358–5367 (2020). [PubMed: 32816951]
15. Diab A et al. , 1053PD - A first-in-human (FIH) study of PF-04518600 (PF-8600) OX40 agonist in adult patients (pts) with select advanced malignancies. Ann Oncol 27 Suppl 6, vi361 (2016).
16. Infante J et al. , A phase Ib dose escalation study of the OX40 agonist MOXR0916 and the PD-L1 inhibitor atezolizumab in patients with advanced solid tumors. J Clin Oncol 34 Suppl 15, 101 (2016).
17. Gutierrez M et al. , OX40 Agonist BMS-986178 Alone or in Combination With Nivolumab and/or Ipilimumab in Patients With Advanced Solid Tumors. Clin Cancer Res 27, 460–472 (2021). [PubMed: 33148673]
18. Shrimali RK et al. , Concurrent PD-1 Blockade Negates the Effects of OX40 Agonist Antibody in Combination Immunotherapy through Inducing T-cell Apoptosis. Cancer Immunol Res 5, 755–766 (2017). [PubMed: 28848055]
19. Messenheimer DJ et al. , Timing of PD-1 Blockade Is Critical to Effective Combination Immunotherapy with Anti-OX40. Clin Cancer Res 23, 6165–6177 (2017). [PubMed: 28855348]
20. Schalper KA et al. , Objective measurement and clinical significance of TILs in non-small cell lung cancer. J Natl Cancer Inst 107, (2015).
21. Velcheti V et al. , Programmed death ligand-1 expression in non-small cell lung cancer. Lab Invest 94, 107–116 (2014). [PubMed: 24217091]
22. Datar I et al. , Expression Analysis and Significance of PD-1, LAG-3, and TIM-3 in Human Non-Small Cell Lung Cancer Using Spatially Resolved and Multiparametric Single-Cell Analysis. Clin Cancer Res 25, 4663–4673 (2019). [PubMed: 31053602]
23. Carvajal-Hausdorf DE et al. , Objective, domain-specific HER2 measurement in uterine and ovarian serous carcinomas and its clinical significance. Gynecol Oncol 145, 154–158 (2017). [PubMed: 28196634]
24. Broz ML et al. , Dissecting the tumor myeloid compartment reveals rare activating antigen-presenting cells critical for T cell immunity. Cancer Cell 26, 638–652 (2014). [PubMed: 25446897]
25. Jimeno A et al. , Abstract CT032: A phase 1/2, open-label, multicenter, dose escalation and efficacy study of mRNA-2416, a lipid nanoparticle encapsulated mRNA encoding human OX40L,

for intratumoral injection alone or in combination with durvalumab for patients with advanced malignancies. Cancer Res 80 Suppl 16, (2020).

26. Hewitt SL et al. , Durable anticancer immunity from intratumoral administration of IL-23, IL-36gamma, and OX40L mRNAs. Sci Transl Med 11, (2019).
27. Wculek SK et al. , Dendritic cells in cancer immunology and immunotherapy. Nat Rev Immunol 20, 7–24 (2020). [PubMed: 31467405]
28. Massarelli E et al. , High OX-40 expression in the tumor immune infiltrate is a favorable prognostic factor of overall survival in non-small cell lung cancer. J Immunother Cancer 7, 351 (2019). [PubMed: 31843013]
29. Shibahara I et al. , OX40 ligand expressed in glioblastoma modulates adaptive immunity depending on the microenvironment: a clue for successful immunotherapy. Mol Cancer 14, 41 (2015). [PubMed: 25744203]
30. Xie K et al. , OX40 expression in hepatocellular carcinoma is associated with a distinct immune microenvironment, specific mutation signature, and poor prognosis. Oncoimmunology 7, e1404214 (2018). [PubMed: 29632718]
31. He Y et al. , OX40 and OX40L protein expression of tumor infiltrating lymphocytes in non-small cell lung cancer and its role in clinical outcome and relationships with other immune biomarkers. Transl Lung Cancer Res 8, 352–366 (2019). [PubMed: 31555511]
32. Kvarnhammar AM et al. , The CTLA-4 x OX40 bispecific antibody ATOR-1015 induces anti-tumor effects through tumor-directed immune activation. J Immunother Cancer 7, 103 (2019). [PubMed: 30975201]
33. Schalper KA et al. , Differential Expression and Significance of PD-L1, IDO-1, and B7-H4 in Human Lung Cancer. Clin Cancer Res 23, 370–378 (2017). [PubMed: 27440266]
34. Nagy A, Munkacsy G, Gyorffy B, Pancancer survival analysis of cancer hallmark genes. Sci Rep 11, 6047 (2021). [PubMed: 33723286]

TRANSLATIONAL RELEVANCE

Multiple OX40/OX40L pathway modulators are being tested clinically as immunostimulatory anti-cancer agents. However, the expression and clinical significance of the OX40/OX40L pathway in human malignancies is not well understood. Using quantitative and spatially-resolved analysis of >600 individual non-small cell lung carcinomas (NSCLCs) from three independent cohorts, we found frequent expression of OX40 protein associated with a favorable immune microenvironment contexture. OX40L protein was uncommonly detected in lung malignancies and its expression was consistently associated with better survival. Similar associations were observed in a cohort of primary uterine/ovarian serous malignancies. As a means to augment OX40L expression lacking in the tumor microenvironment, we show proof-of-concept evidence that intratumoral administration of exogenous OX40L mRNA encapsulated in lipid nanoparticles (LNPs) leads to increased local OX40L protein levels in cancer. Together, our results expand the understanding of the OX40/OX40L pathway in human tumors and support the local modulation of OX40L as a candidate therapeutic intervention.

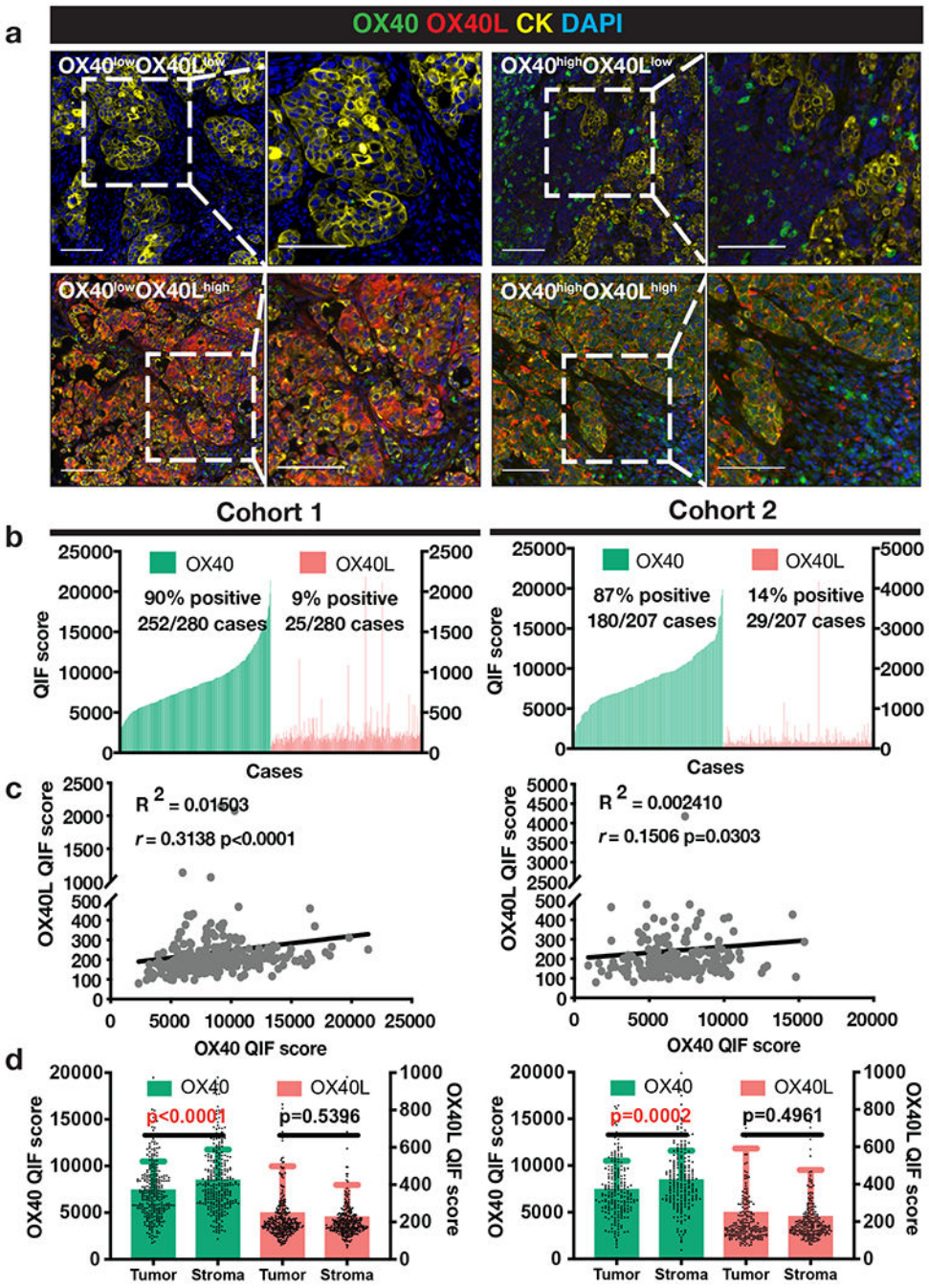

Figure 1. Distribution and localization of OX40 and OX40L expression in human NSCLC.

(a) Representative multiplexed quantitative immunofluorescence (QIF) micrographs of human NSCLC cases with varying expression levels of OX40 (green) and OX40L (red). Cytokeratin (CK) (yellow) marks tumor epithelial cells and DAPI (blue) marks all nuclei. Scale bar=100 μm. (b) QIF score distributions of OX40 and OX40L arranged by increasing order of OX40 expression in Cohort 1 (N=280) and Cohort 2 (N=207) of human NSCLC cases. QIF scores on the left Y-axis refer to OX40 and on the right to OX40L. (c) Spearman correlation between total OX40 and OX40L levels in Cohorts 1 and 2. (d) OX40 and

OX40L QIF scores (mean ± SD) in Cohorts 1 and 2 across tumor and stroma compartments. Statistical analysis by Mann-Whitney test.

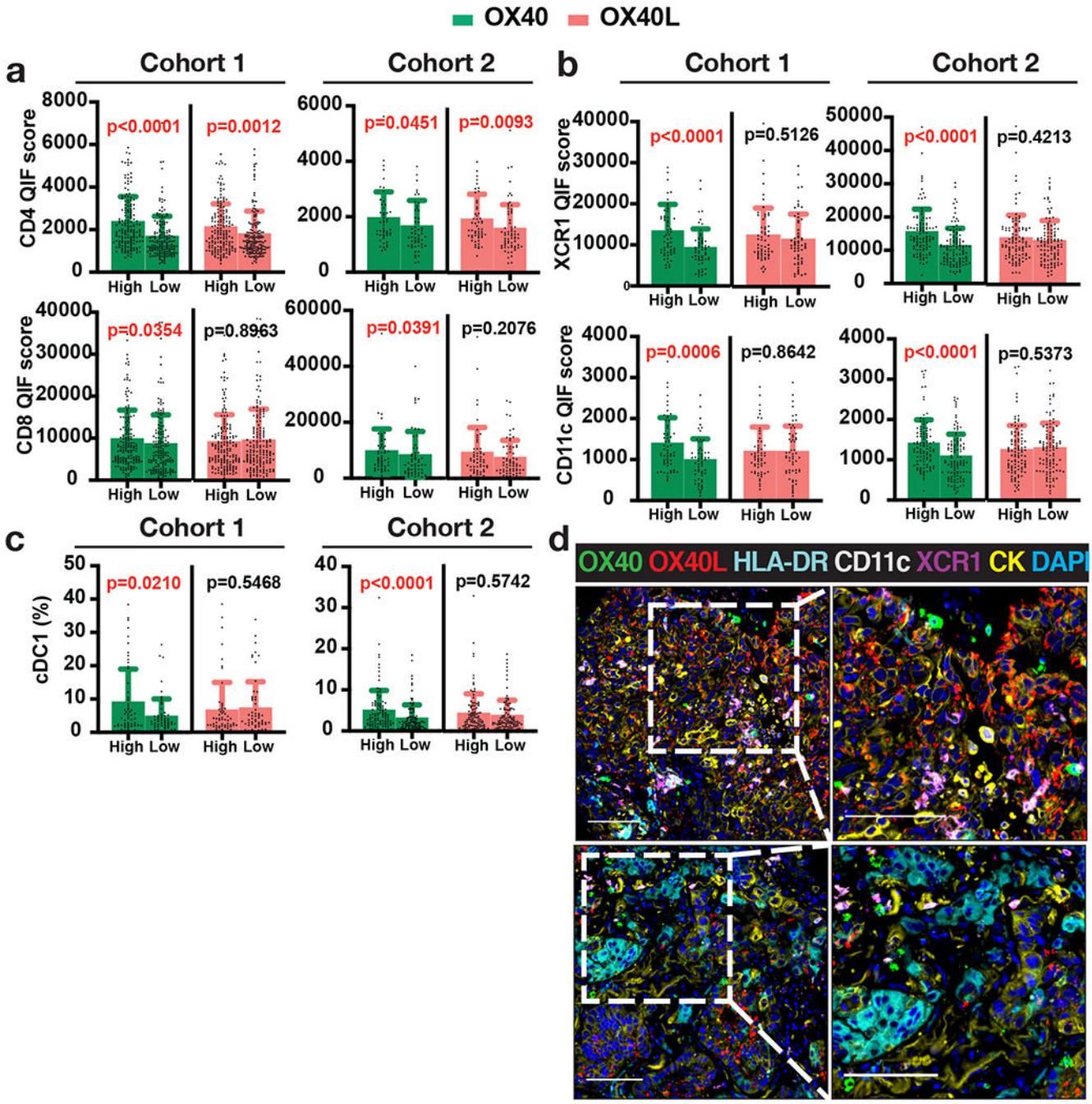

Figure 2. Association of OX40 and OX40L levels with immune markers.

(a-c) Quantification of immune markers in Cohorts 1 and 2 divided into OX40 or OX40L High and Low groups using median cut-point: QIF scores (mean ± SD) of (a) TIL markers CD4 and CD8, (b) cDC1 markers XCR1 and CD11c, and (c) percentages of cDC1 ($XCR1^+$ $CD11c^+$ $HLA\text{-}DR^+$) (number of cDC1/total number of cells). Statistical analysis by Mann-Whitney test. (d) Representative images of cases with OX40/OX40L-high levels, marked by high infiltration of cross-presenting dendritic cells positive for markers XCR1, CD11c, and

HLA-DR (upper panel), and OX40/OX40L-low levels accompanied by low abundance of XCR1- and CD11c-expressing cells (lower panel).

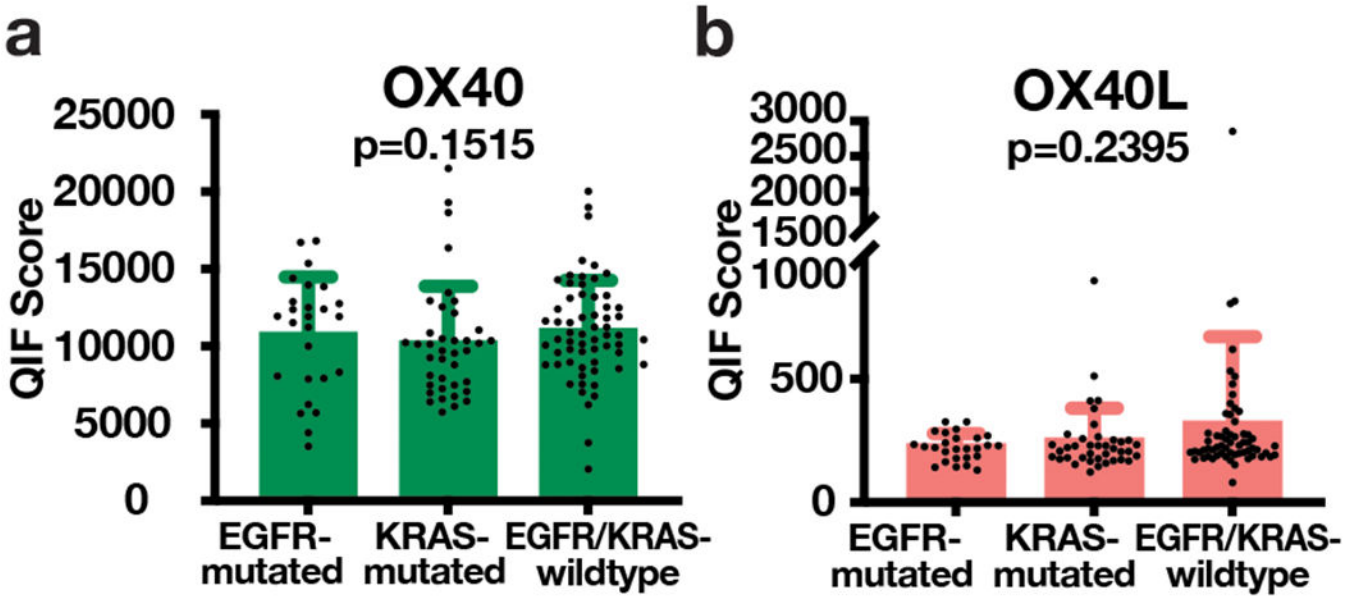

Figure 3. Association of OX40 and OX40L with EGFR and KRAS mutations.

(a) OX40 and (b) OX40L QIF scores (mean ± SD) plotted for EGFR-mutated, KRAS-mutated, and EGFR/KRAS-wildtype cases. Statistical analysis by Kruskal-Wallis test.

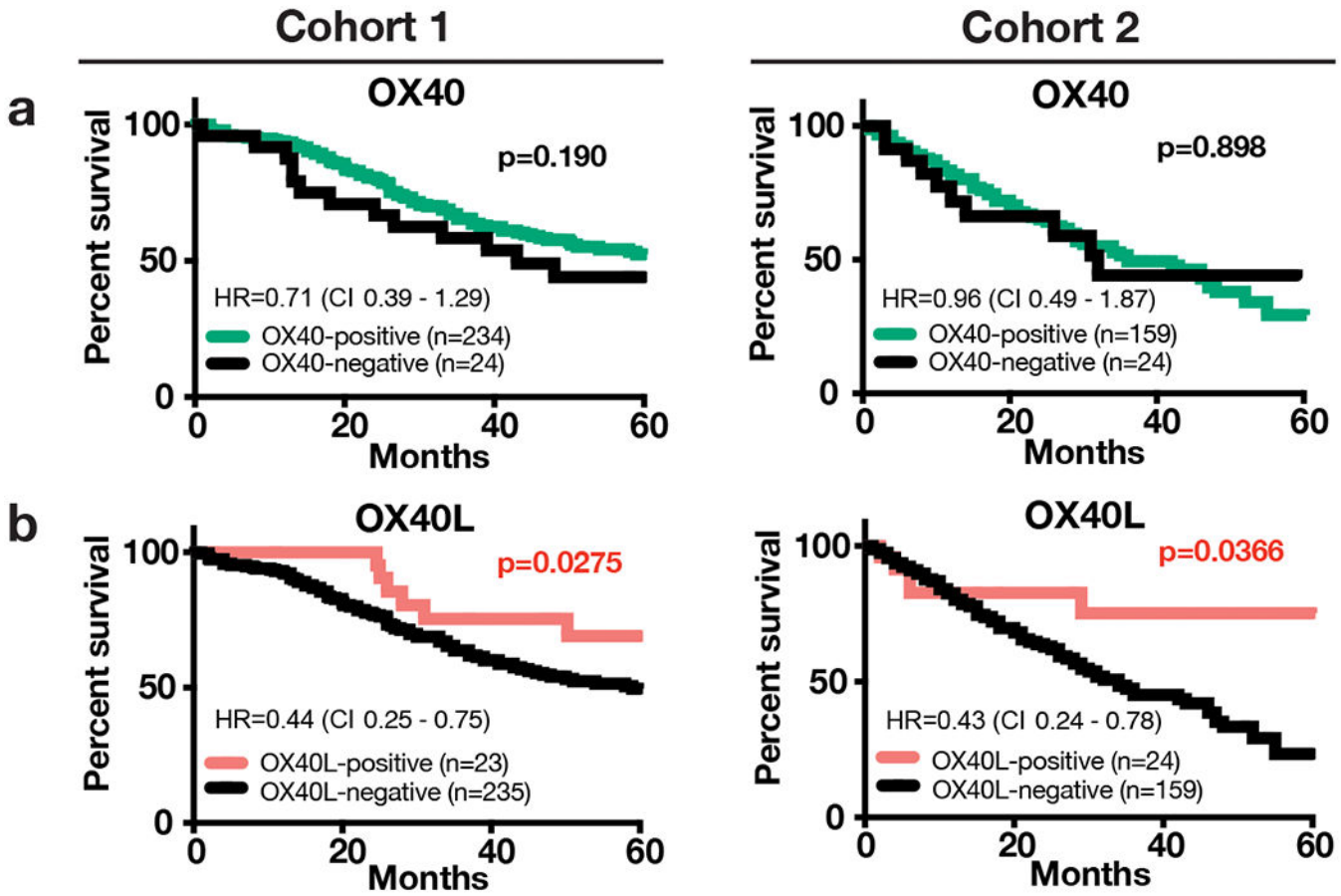

Figure 4. Association of OX40 and OX40L with survival.

Kaplan-Meier graphical analysis showing the association of OX40 (a) and OX40L (b) with 5-year overall survival in Cohorts 1 and 2. Statistical analysis performed by Mantel-Cox/ Log-rank test reporting Hazard ratios (HR) (log-rank) and confidence intervals (CI).

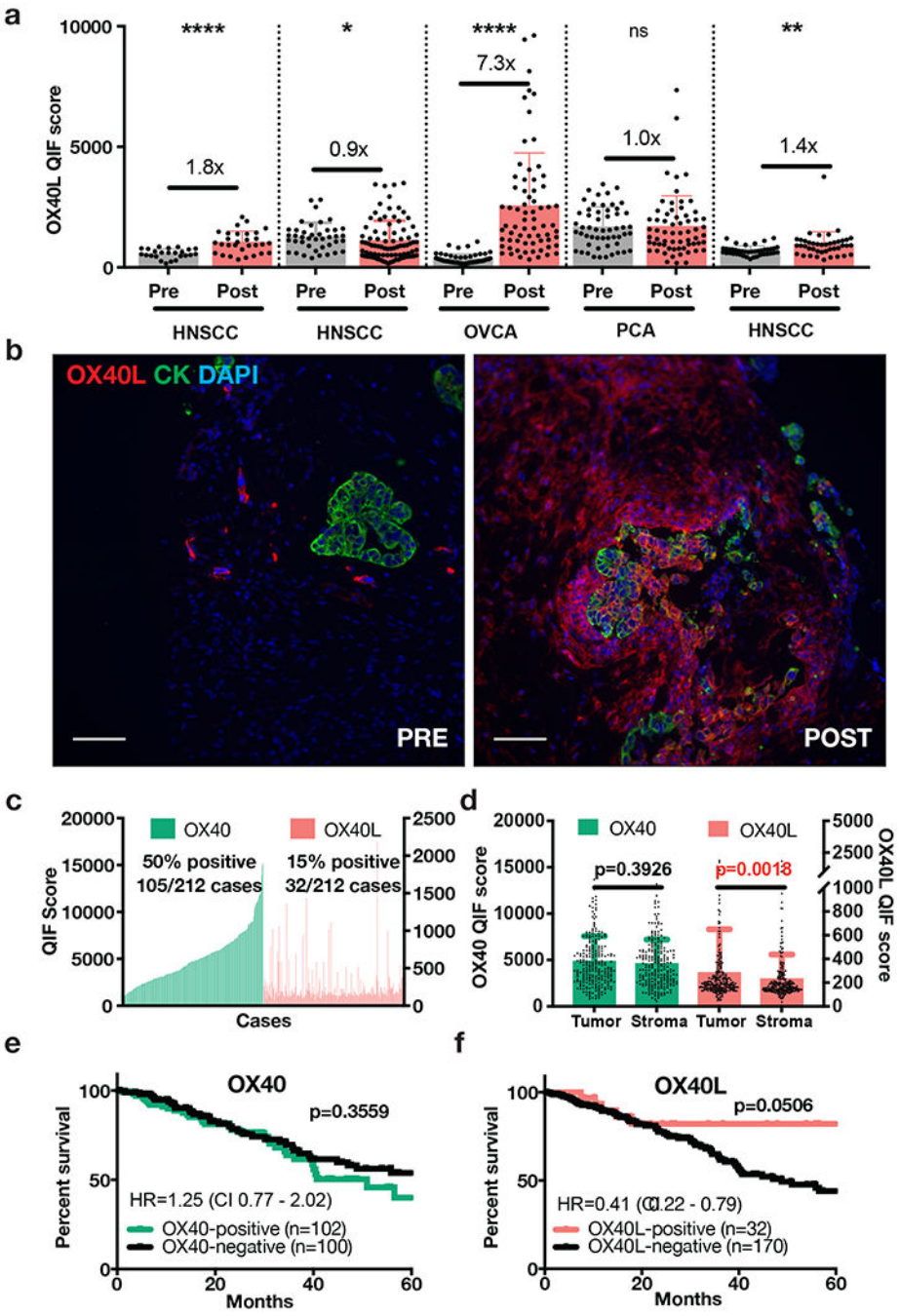

Figure 5. OX40L detection in patient biopsies pre- and post-exogenous OX40L injection, and expression of the OX40 pathway and survival in patients with primary serous carcinomas.

(a) OX40L QIF scores for pre- and post-exogenous OX40L (mRNA-2416) injection biopsies of patients with HNSCC (head-and-neck squamous cell carcinoma), OVCA (ovarian cancer), and PCA (prostate cancer). Post- treatment biopsies were collected 24 to 48 hours after injection of mRNA-2416. Also shown are the protein level changes based on pre/post-treatment scores. Each dot indicates the OX40L protein QIF score obtained from each individual 20X field of view in the whole tissue section specimen. Statistical analysis performed by unpaired t-test or Mann-Whitney test. ****p<0.0001. **p<0.01. *p<0.05.

(b) Pre- and post-administration biopsies of LNP-formulated mRNA encoding OX40L (mRNA-2416) in patient with ovarian cancer (QIF scores shown in Figure 5a) where OX40L was detected at the highest levels 48 hours after treatment. Scale bar=100 μm.
(c) QIF score distributions of OX40 and OX40L arranged by increasing order of OX40 expression in a retrospective cohort of 212 human primary serous carcinomas. QIF scores on the left Y-axis refer to OX40 and on the right to OX40L.
(d) OX40 and OX40L QIF scores (mean ± SD) in tumor and stromal compartments. Statistical analysis by Mann-Whitney test.
(e-f) Kaplan-Meier analysis of the 5-year overall survival in human primary uterine/ovarian serous carcinomas with high or low OX40 (e) and OX40L (f) protein levels. Statistical analysis performed by Mantel-Cox/Log-rank test reporting Hazard ratios (HR) (log-rank) and confidence intervals (CI).

Table 1.

Association of OX40 positivity with clinicopathologic variables. Statistical analysis by Pearson Chi-Square test.

Variable	COHORT 1 (N=280)			COHORT 2 (N=207)		
	OX40-positive	OX40-negative	p-value	OX40-positive	OX40-negative	p-value
	252 (90%)	28 (10%)		180 (87%)	27 (13%)	
Age						
≤ 70	154 (92%)	14 (8%)	0.325	130 (87%)	20 (13%)	0.607
> 70	96 (88%)	13 (12%)		35 (90%)	4 (10%)	
Gender						
Male	103 (87%)	16 (13%)	0.075	142 (87%)	22 (13%)	0.727
Female	146 (93%)	11 (7%)		21 (84%)	4 (16%)	
Stage						
Stage I-II	188 (90%)	21 (10%)	0.903	93 (84%)	18 (16%)	0.255
Stage III-IV	57 (90%)	6 (10%)		69 (90%)	8 (10%)	
Histology						
ADC	153 (91%)	15 (9%)		65 (90%)	7 (10%)	0.330
SCC	47 (89%)	6 (11%)	0.744	75 (82%)	16 (18%)	
Others	43 (88%)	6 (12%)		23 (88%)	3 (12%)	
Smoking status						
Non/former smoker	125 (89%)	16 (11%)	0.479	16 (89%)	2 (11%)	0.761
Smoker	115 (91%)	11 (9%)		126 (86%)	20 (11%)	

Table 2.

Association of OX40L positivity with clinicopathologic variables. Statistical analysis by Pearson Chi-Square test.

Variable	COHORT 1 (N=280)			COHORT 2 (N=207)		
	OX40L-positive	OX40L-negative	p-value	OX40L-positive	OX40L-negative	p-value
	25 (9%)	255 (91%)		29 (14%)	178 (86%)	
Age						
≤ 70	16 (10%)	152 (90%)	0.719	23 (15%)	127 (85%)	0.420
> 70	9 (8%)	100 (92%)		4 (10%)	35 (90%)	
Gender						
Male	12 (10%)	107 (90%)	0.605	22 (13%)	142 (87%)	0.846
Female	13 (8%)	144 (92%)		3 (12%)	22 (88%)	
Stage						
Stage I-II	21 (10%)	188 (90%)	0.373	14 (13%)	97 (87%)	0.740
Stage III-IV	4 (6%)	59 (94%)		11 (14%)	66 (86%)	
Histology						
ADC	15 (9%)	153 (91%)		11 (15%)	61 (85%)	
SCC	8 (15%)	45 (85%)	**0.023**	13 (14%)	78 (86%)	0.309
Others	0 (0%)	49 (100%)		1 (4%)	25 (96%)	
Smoking status						
Non/former smoker	9 (6%)	132 (94%)	0.077	1 (6%)	17 (94%)	0.300
Smoker	16 (13%)	110 (87%)		21 (14%)	125 (86%)	